A Micromechanical Theory of Flow in Pulmonary Alveolar Sheet

Z. Zhong [1], Y. Dai[1,2], C. C. Mei [3] and P. Tong[1,4]

Abstract: In this paper we reexamine the sheet-flow model proposed by Fung and Sobin (1969) for blood flow in capillaries in the pulmonary alveoli from micromechanical point of view. The pulmonary alveolar capillary is assumed to be two parallel membranes connected by periodic tissue posts. Blood is spread out into the very thin layer or sheet between the two membranes. The pulmonary alveolar sheet thus has a microstructure of hexagonal cells. A two-scale theory of homogenization is used to establish the canonical equations for the unit cell. The microscale solution is obtained by means of finite element method and the macroscopic pressure/discharge relationship for the flow in the pulmonary alveolar sheet is found through an average over the unit cell. The influence of cell geometry on the permeability and geometric friction factor of the cell are discussed through numerical examples.

The tissue posts have a significant effect on the flow resistance. Reducing either the post diameter or the vascular space tissue ratio will reduce permeability. For the post configuration considered, with a post volume of 4.5% of the cell, the ratio of permeability to that of Couette flow (K_{11}/K^0) changes from 0.8 to about 0.3 when the sheet gap to post diameter ratio (h/a) increases from 1 to 5. The reduction in permeability is even more pronounce with denser posts. At $h/a = 5$, K_{11}/K^0 is only about 0.3 for the post volume of 4.5% of the cell. When the post volume increases to 20% of the cell, K_{11}/K^0 drops to 0.05.

keyword: blood flow, pulmonary alveolar sheet, sheet-flow model, permeability, micromechanical theory, homogenization

[1] Department of Mechanical Engineering, Hong Kong University of Science and Technology, Hong Kong

[2] Department of Engineering Mechanics & Technology, Tongji University, Shanghai 200092, P. R. China

[3] Civil Engineering Department, MIT, Cambridge, MA 02139, USA

[4] corresponding author.
 Tel: +852-2358-7202; fax: +852-2358-1543.
 E-mail address: pintong@ust.hk

1 Introduction

The function of lung is to oxygenate the blood and remove carbon dioxide by diffusion and chemical reactions, and for this purpose blood is spread out into very thin layers or sheets so that the blood-gas interfacial area becomes very large. Each sheet of blood, bounded by two membranes, forms an inter-alveolar septum. Several billion septa form a space structure like a honeycomb or a bowl of soap bubbles. The smallest unit of air space bounded by inter-alveolar septa is called the alveolus.

The close interconnectivity among capillaries in the inter-alveolar septa prompted Fung and Sobin (1969) to propose a sheet-flow model, which consists of two elastic and narrowly spaced membranes connected by a uniform array of tissue posts. Forced by higher pressure in the arteriole, blood plasma and red blood cells enter the sheet and pass through the tortuous space among the posts and exit to the venule. Because of the membrane elasticity, the gap between the two membranes can expand with increasing blood pressure. The flow speed is typically low, so the fluid mechanical problem is that of a flow through a deformable porous medium. Since the exchange of oxygen or carbon dioxide between air in the alveoli and blood in the alveolar sheet depends on the blood flow, the first fluid mechanical task is to determine the pressure/discharge relationship on the macroscale. The second task is to model the gas exchange across the alveolar walls and in the plasma and red blood cells. In either task simplified models can help qualitative understanding and quantitative estimation.

In the theoretical model for pure blood plasma flow without red blood cells, Fung and Sobin (1969) began with Dracy' law and the macroscopic viewpoint of the characteristics of groundwater seepage, in that only the average quantities such as pressure and the average seepage velocities (U_x, U_y) parallel to plane of the walls are considered. A relation between the local pressure gradient and the seepage velocity is

$$\frac{\partial p}{\partial x_i} = -\frac{\mu \eta f_{ij} U_j}{h^2} \tag{1}$$

where μ is the apparent viscosity of blood and η is an empirical factor depending weakly on the ratio of sheet thickness h to the interpostal distance L(for all practical purposes, η can be taken as 12); f_{ij} is a function of the sheet geometry, which is called geometric friction factor (Fung, 1997). With an additional approximation on the wall elasticity that

$$h = \begin{cases} h_0 + \alpha(p - p_0) & p > p_0 \\ 0 & p < p_0 \end{cases} \tag{2}$$

where α is called the compliance coefficient of the pulmonary capillary bed, the governing differential equation for blood flow is derived as

$$\frac{1}{\mu}\left\{ \frac{\partial}{\partial x}\left(\frac{h^3}{\eta f_x}\frac{\partial p}{\partial x} \right) + \frac{\partial}{\partial y}\left(\frac{h^3}{\eta f_y}\frac{\partial p}{\partial y} \right) \right\} = \frac{\partial h}{\partial t} + 2\frac{\kappa}{\rho}(p - p^*), \tag{3}$$

where κ is the filtration coefficient, p^* is the pressure in the alveolar space, and f_{ij} is taken to be a diagonal tensor ($f_x = f_{11}, f_y = f_{22}$).

The sheet-flow model proposed by Fung and Sobin (1969) is especially advantageous for the description of capillary elasticity. Theoretical predictions based on the sheet-flow model have shown very good agreement with experimental measurements over a wide range of conditions in steady flow (Zhuang, Fung and Yen, 1983; Yen, Zhuang, Fung and Zeng, 1984; Fung and Yen, 1986; Yen and Sobin, 1986) and in pulsatile flow (Fung, 1972; Gan and Yen, 1994; Olman, Gan, Yen, Villespin, Maxwell, Pedersen, Konopka, Debes and Moser, 1994; Huang, Tian, Gao and Yen, 1998; Gao, Huang and Yen, 2000). The geometric friction factor f_{ij} is needed to be exactly determined before we study the steady flow ($\partial h/\partial t = 0$) or the pulsatile flow ($\partial h/\partial t \neq 0$) using Eq. (3). The geometric friction factor f_{ij} have been experimentally obtained (Yen and Fung, 1973) or theoretically approximated (Lee, 1969).

In this paper we reexamine the sheet-flow model of Fung and Sobin (1969) from the micromechanical point of view and calculate the geometric friction factor by a numerical approach. The pulmonary alveolar sheet is assumed to be of a periodic microstructure with hexagonal cells and then a two-scale theory of homogenization is used to establish the canonical equations for the unit cell. The microscale solution is obtained by means of finite element method and then the macroscopic pressure/discharge relationship for the flow in the pulmonary alveolar sheet is found through an average over the unit cell. We find that the posts have a strong nonlinear effect on the flow resistance. When h/a is large, the flow resistance is mainly from the posts and the permeability reduces rapidly as h/a increases. For the post configuration considered, at the post volume of 4.5% of the cell and $h/a = 5$, the permeability is only about 30% of the Couette flow. The effect is even more pronounce for the sheet flow with denser posts. At the post volume of 20% and $h/a = 5$, the permeability drops to about 5% of the Couette flow.

2 Formulation

In this paper, to simplify writing, the repetition of a subscript in a term will denote a summation with respect to that subscript from 1 to 3 unless specified otherwise. We consider the flow of pure plasma so that the Navier-Stokes equations for incompressible Newtonian fluids are appropriate

$$\frac{\partial u_i}{\partial x_i} = 0 \tag{4}$$

$$\rho\frac{\partial u_i}{\partial t} + \rho u_j\frac{\partial u_i}{\partial x_j} = -\frac{\partial p}{\partial x_i} + \mu\frac{\partial^2 u_i}{\partial x_j \partial x_j} \tag{5}$$

where μ is the viscosity and ρ the density of pure plasma. Let ω^{-1} be the time scale, U the velocity scale, ΔP the scale of pressure variations, l the typical inter-postal distance, and L the size of the alveolar sheet. Then for low speed flow we expect the pressure gradient to be comparable to the viscous stress, hence

$$\frac{\Delta P}{L} \sim \frac{\mu U}{l^2}$$

The ratios of acceleration and convective inertia to the viscous stress are

$$\frac{\rho \frac{\partial u_i}{\partial t}}{\mu \frac{\partial^2 u_i}{\partial x_j \partial x_j}} \sim \frac{\rho \omega l^2}{\mu} = \frac{\omega l^2}{\nu} = \left(\frac{l}{\delta}\right)^2 = W_0^2,$$

$$\frac{\rho u_j \frac{\partial u_i}{\partial x_j}}{\mu \frac{\partial^2 u_i}{\partial x_j \partial x_j}} \sim \frac{\rho U l}{\mu} = \frac{U l}{\nu} = Re,$$

(i not summed) where W_0 is the Womersley number and Re the Reynolds number. Taking for estimate

$$l = 10^{-3}\text{cm}, \quad \nu = 10^{-2}\text{cm}^2/\text{s}, \quad \omega = 2\pi/\text{s}, \quad U = 0.1\text{cm/s},$$

we get $W_0 \sim O(10^{-2}) << 1$ and $Re = 10^{-2} << 1$. Normalizing all coordinates by l, we then have

$$\frac{\frac{\partial p}{\partial x_i}}{\mu \frac{\partial^2 u_i}{\partial x_j \partial x_j}} \sim \frac{\Delta P l}{\mu U} = \frac{\mu U}{l^2} \frac{L l}{\mu U} = \frac{L}{l} >> 1, \text{ (i not summed)}.$$

Since $L \sim O(1\text{cm})$, we define a small parameter $\varepsilon = l/L << 1$, and assume $Re = O(\varepsilon)$ and $W_0 = O(\varepsilon)$. For ease of identification, we rewrite Eq. (5) according to the relative magnitude of respective terms (using ε to express the relative magnitude) as (Mei, Auriault and Ng, 1996):

$$\varepsilon^3 \rho \frac{\partial u_i}{\partial t} + \varepsilon^2 \rho u_j \frac{\partial u_i}{\partial x_j} = -\frac{\partial p}{\partial x_i} + \varepsilon \mu \frac{\partial^2 u_i}{\partial x_j \partial x_j} \tag{6}$$

Let the posts be cylindrical and bounded by Γ. We assume, by ignoring their transverse deformation,

$$u_i = 0 \quad \text{on} \quad \Gamma \tag{7}$$

Let us define the surfaces $F_\mp = z \mp h(x,y,t)/2$. The lower and upper membrane surfaces correspond to $F_\mp = 0$. We allow seepage at these surfaces and express the difference between the normal components of the blood velocity $\mathbf{u}$ and the membrane velocity $\mathbf{q}$ in terms of the pressure difference on two sides of the alveolar membrane. According to Starling's hypothesis, the filtration is

$$\rho(\mathbf{u} - \mathbf{q}) \cdot \mathbf{n} = \pm \kappa(p - p^*) \quad \text{at } z = \pm h/2, \tag{8}$$

where κ is the filtration coefficient and p^* is the pressure of the alveoli.

Equation (8) can be a nonlinear function of h. The normal velocity of the membrane is

$$\mathbf{q} \cdot \mathbf{n} = \frac{\mathbf{q} \cdot \nabla F}{|\nabla F|} = -\frac{\partial F/\partial t}{|\nabla F|}, \tag{9}$$

in which we have made use of the kinematic condition on the membrane

$$\frac{\partial F}{\partial t} + \mathbf{q} \cdot \nabla F = 0 \tag{10}$$

It follows from Eq. (8) that

$$\frac{\partial F/\partial t}{|\nabla F|} + \frac{\mathbf{u} \cdot \nabla F}{|\nabla F|} = \pm \frac{\kappa}{\rho}(p - p^*) \tag{11}$$

or

$$\pm \frac{1}{2}\left(-\frac{\partial h}{\partial t} - u_x h_x - u_y h_y\right) + u_z = \\ \pm \frac{\kappa}{\rho}(p - p^*)\sqrt{1 + \frac{1}{4}\left(h_x^2 + h_y^2\right)} \tag{12}$$

on the membrane $z = \pm h/2$, where $u_x = u_1, u_y = u_2, h_x = \partial h/\partial x, h_y = \partial h/\partial y$. As will be shown shortly, the leading order of the blood pressure varies according to the macro length scale L of the sheet. We assume the same for the longitudinal variation of h in order to be consistent with Eq. (2). This amounts to neglecting the local indentations at places where the posts join the sheet. Since $O(h) = l$, we have

$$\frac{\partial h/\partial t}{u_z} = \frac{\omega l}{U} = \frac{W_0^2}{Re} = O(\varepsilon)$$

Also we assume that filtration through the membrane is slow so that $\kappa(p - p^*) = O(\partial h/\partial t)$. It follows that, on $z = \pm h/2$, Eq. (12) can be rewritten according to the relative magnitude as follows:

$$u_z = \pm \frac{\varepsilon}{2}\left(\frac{\partial h}{\partial t} + u_x h_x + u_y h_y\right) \\ \pm \varepsilon \frac{\kappa}{\rho}(p - p^*)\sqrt{1 + \frac{\varepsilon^2}{4}\left(h_x^2 + h_y^2\right)} \tag{13}$$

It can be found in the next section that the assumption, $\kappa(p - p^*) = O(\partial h/\partial t)$, will lead to the derivation of the governing equation for blood flow, Eq. (3) or Eq. (33).

3   Two-scale expansions

The important characteristics of the above problem are the existence of two vastly different length scales: the microscale l, which characterizes the typical inter-postal distance, and the macroscale L, which characterizes the size of the alveolar sheet. The perturbation method of multiple scales is particularly suitable for problems involving contrasting scales (Mei, Auriault and Ng, 1996; Tong and Mei, 1992; Bush, 1992; Kalamkarov, 1992; Parton and Kudryavtsev, 1993; Carvelli, Maier and Gastaldi, 2000; Michel, Moulinec and Suquet, 2000). Let $\varepsilon = l/L << 1$, we introduce two coordinates defined by

$$\mathbf{x} = (x, y, z) \quad \mathbf{X} = (\varepsilon x, \varepsilon y, z) \tag{14}$$

where the lower-case and upper-case coordinates represent microscale (fast) and macroscale (slow) variations respectively. The two-scale expansions are assumed as follows:

$$\begin{aligned} u_i &= u_i^{(0)} + \varepsilon u_i^{(1)} + \varepsilon^2 u_i^{(2)} + \cdots \\ p &= p^{(0)} + \varepsilon p^{(1)} + \varepsilon^2 p^{(2)} + \cdots \end{aligned} \tag{15}$$

where

$$u_i^{(n)} = u_i^{(n)}(\mathbf{x}, \mathbf{X}, t), \quad p^{(n)} = p^{(n)}(\mathbf{x}, \mathbf{X}, t), \quad n = 1, 2, 3.$$

Substituting (15) into the continuity equation, Eq. (4), we obtain the perturbation equations for orders $O(1)$, $O(\varepsilon)$, $O(\varepsilon^2)$,..., respectively:

$$\frac{\partial u_i^{(0)}}{\partial x_i} = 0, \tag{16a}$$

$$\frac{\partial u_i^{(1)}}{\partial x_i} + \frac{\partial u_i^{(0)}}{\partial X_i} = 0, \tag{16b}$$

$$\frac{\partial u_i^{(2)}}{\partial x_i} + \frac{\partial u_i^{(1)}}{\partial X_i} = 0, \tag{16c}$$

....

Similarly, from the momentum equation, Eq. (6), we get the perturbation equations of the corresponding orders

$$\frac{\partial p^{(0)}}{\partial x_i} = 0, \tag{17a}$$

$$\frac{\partial p^{(1)}}{\partial x_i} + \frac{\partial p^{(0)}}{\partial X_i} - \mu \frac{\partial^2 u_i^{(0)}}{\partial x_j \partial x_j} = 0, \tag{17b}$$

$$\frac{\partial p^{(2)}}{\partial x_i} + \frac{\partial p^{(1)}}{\partial X_i} - \mu \frac{\partial}{\partial x_j}\left(\frac{\partial u_i^{(1)}}{\partial x_j} + 2\frac{\partial u_i^{(0)}}{\partial X_j} \right) + \rho u_j^{(0)} \frac{\partial u_i^{(0)}}{\partial x_j} = 0, \tag{17c}$$

....

All velocity components vanish on the walls of all posts

$$u_i^{(0)} = u_i^{(1)} = u_i^{(2)} = \cdots = 0, \quad i = 1, 2, 3 \quad \text{on} \quad \Gamma. \tag{18}$$

The boundary conditions on the membranes will be applied on $z = \pm h/2$. Thus the horizontal components vanish at all orders

$$u_i^{(0)} = u_i^{(1)} = u_i^{(2)} = \cdots = 0 \quad i = 1, 2, \quad z = \pm h/2 \tag{19}$$

As for the vertical components, we expand Eq. (13) and obtain

$$\begin{aligned} u_z^{(0)} &= 0 \\ \pm u_z^{(1)} &= \frac{1}{2}\frac{\partial h}{\partial t} + \frac{\kappa}{\rho}(p^{(0)} - p^*) \\ \pm u_z^{(2)} &= \frac{\kappa}{\rho} p^{(1)} \end{aligned} \tag{20}$$

....

on $z = \pm h/2$.

Note that Eqs. (6) and (13) include time dependent terms, while Eqs. (17a) – (17c) do not. This is because the time dependent term is of the order $O(\varepsilon^3)$ and does not appear in the perturbation equations of lower orders.

Now we can examine the perturbation problems at successive orders.

4   Macroscale equations

From Eq. (17a) we get at $O(1)$

$$p^{(0)} = p^{(0)}(\mathbf{X}, t) \tag{21}$$

implying that at the leading order pressure is just the averaged pressure independent of the microscale coordinates.

At the order $O(\varepsilon)$, $u_i^{(0)}$ with $i = 1, 2, 3$ and $p^{(1)}$ are governed by Eqs. (16a) and (17b), subject to the non-slip boundary condition on $z = \pm h/2$ and Γ. In addition, we define a unit cell Ω and require Ω-periodicity for $u_i^{(0)}$ and $p^{(1)}$. Because of the linearity of (17b), $u_i^{(0)}$ and $p^{(1)}$ can be assumed as (Mei, Auriault and Ng, 1996)

$$u_i^{(0)} = -k_{ij}\frac{\partial p^{(0)}}{\partial X_j} \tag{22}$$

and

$$p^{(1)} = -A_j\frac{\partial p^{(0)}}{\partial X_j} \tag{23}$$

where k_{ij} and A_j are Ω-periodic and unknown functions of x_i and X_i. It follows from (16a) and (17b) that k_{ij} and A_j must satisfy

$$\frac{\partial k_{ij}}{\partial x_i} = 0 \tag{24}$$

$$\mu\frac{\partial^2 k_{ij}}{\partial x_k \partial x_k} - \frac{\partial A_j}{\partial x_i} = -\delta_{ij} \tag{25}$$

in the unit cell ($x_i \in \Omega$), for $i = 1, 2, 3$ and $j = 1, 2$. The boundary conditions on the boundaries $z = \pm h/2$ and Γ are

$$k_{ij} = 0. \tag{26}$$

Equations (24) and (25) constitute a set of Stokes problems in Ω.

The solution for A_j is unique only to a constant. Thus we impose further

$$\langle A_j \rangle = 0 \tag{27}$$

where $\langle f \rangle$ denotes the cell average of f defined as

$$\langle f \rangle = \frac{1}{S_b h}\int_{-h/2}^{h/2} dz \iint_{S_b} f\, dx dy \tag{28}$$

in which f can be a scalar, vector or tensor, and S_b is the base area of Ω. This condition ensures that $p^{(0)}$ is the average pressure with error at most of $O(\varepsilon^2)$.

Once unknown functions k_{ij} and A_j are determined, we obtain Darcy' law

$$\left\langle u_i^{(0)} \right\rangle = -K_{ij}\frac{\partial p^{(0)}}{\partial X_j}, \tag{29}$$

where

$$K_{ij} = \langle k_{ij} \rangle \tag{30}$$

is the permeability.

It can be shown that

$$\iiint_{\Omega}\frac{\partial u_i^{(0)}}{\partial X_i}d\Omega = \frac{\partial}{\partial X_i}\iiint_{\Omega}u_i^{(0)}d\Omega = S_b\frac{\partial}{\partial X_i}\left(\left\langle u_i^{(0)}\right\rangle h\right), \tag{31a}$$

$$\iiint_{\Omega}\frac{\partial u_i^{(1)}}{\partial x_i}d\Omega = S_b\left[u_z^{(1)}\right]_{-h/2}^{h/2} = S_b\left[\frac{\partial h}{\partial t} + 2\frac{\kappa}{\rho}\left(p^{(0)} - p^*\right)\right], \tag{31b}$$

in which we have accounted for the Ω-periodicity condition of $u_i^{(0)}$ and $u_i^{(1)}$ that

$$\int_{\partial\Omega}\mathbf{n}\cdot\mathbf{u}^{(0)}ds = \int_{\partial\Omega}\mathbf{n}\cdot\mathbf{u}^{(1)}ds = 0,$$

where $\partial\Omega$ is the cross-sectional boundary of Ω at constant z. It follows from Eqs. (16b) and (31b) that

$$-\frac{\partial}{\partial X_i}\left(\langle u_i^{(0)}\rangle h\right) = \frac{\partial h}{\partial t} + 2\frac{\kappa}{\rho}\left(p^{(0)} - p^*\right) \quad . \tag{32}$$

Using Darcy' law Eq. (29), we get

$$\frac{\partial}{\partial X_i}\left(K_{ij}h\frac{\partial p^{(0)}}{\partial X_j}\right) = \frac{\partial h}{\partial t} + 2\frac{\kappa}{\rho}\left(p^{(0)} - p^*\right) \quad . \tag{33}$$

It can be seen that Eqs. (29) and (33) agree with Eqs. (1) and (3) if we express the geometric frictional factor as

$$f_{ij} = \frac{h^2}{\mu\eta}K_{ij}^{-1}, \tag{34}$$

where K_{ij}^{-1} is the inverse of the permeability K_{ij}.

We have now deduced Fung and Sobin' macroscale theory of the flow in capillaries in the pulmonary alveolar sheet from micromechanical point of view. The advantage of the present approach is the theoretical predictability of K_{ij} by solving Eqs. (16a) and (17b) in a unit cell for any periodic geometry. With predicted K_{ij}, one can solve Eq. (34) in the regular manner. Once $p^{(0)}$ is solved, the local velocity field in each cell is known from Eq. (22). Thus aside from the theoretical advantage of deducing the macroscale theory from micromechanical approach, the present technique gives detailed flow information on the microscale.

It can be shown that $K_{ij} = K_{ji}$ and that the quadratic function $K_{ij}x_ix_j$ is always greater than zero for any nonzero x_i, i.e., K_{ij} is positive definite. In general, K_{ij} are not diagonal.

Note that the assumption, $\kappa(p - p^*) = O(\partial h/\partial t)$, lead to the derivation of the governing equation for pulsatile and permeable blood flow, Eq. (3) or Eq. (33).

5   Numerical solution for unit cell

On the microscale, the posts are assumed to be periodically spaced, with a height of h and a circular cross-section of diameter a, as shown in Fig. 1. A local coordinate system is used where the posts are in the $z-$direction. There are a number of ways that the pulmonary alveolar sheet can be divided into periodic unit cells. In the following calculation, we choose a hexagon

with a post at the center as a unit cell Ω. The dimensions of the hexagon can be expressed in terms of post spacing (x_0, y_0):

$$l_1 = \frac{1}{2}\left(y_0 + \frac{x_0^2}{y_0}\right), \quad l_2 = \frac{1}{2}\left(y_0 - \frac{x_0^2}{y_0}\right). \tag{35}$$

The vascular-space tissue ratio (VSTR), defined as the ratio of the vascular lumen volume to the circumscribing volume of the cell (Fung, 1997), can be obtained as

$$\text{VSTR} = 1 - \frac{\pi a^2}{8(l_1 + l_2)x_0} = 1 - \frac{\pi a^2}{8x_0y_0}. \tag{36}$$

We shall determine the permeability K_{ij} by solving Eqs. (16a) and (17b) in the unit cell, with non-slip boundary conditions on the membranes, $z = \pm h/2$ and the wall of the post, Γ. It is difficult to obtain the exact solution to Eqs. (16a) and (17b). Hence, a simple and approximate solution technique will be proposed as follows:

Combining Eqs. (16a) and (17b) leads to

$$\mu(u_{i,jj}^{(0)} - u_{j,ji}^{(0)}) - p_{,i}^{(1)} + F_i = 0, \tag{37}$$

where $(.)_{,j} = \partial(.)/\partial x_j$ and $F_i = -\partial p^{(0)}/\partial X_i$. Note that F_i is independent of the microscale coordinate x_i and that it is to be determined from the macroscale solution.

Equation (37) is the same as the Navier equation for elasticity if μ (the viscosity coefficient) is taken as the shear modulus, F_i as the body force per unit volume, $u_i^{(0)}$ as the displacement and $p^{(1)}$ as the hydrostatic pressure,

$$p^{(1)} = -(\lambda + 2\mu)u_{j,j}^{(0)} = -\frac{2\mu(1 - \nu)}{1 - 2\nu}u_{j,j}^{(0)} \tag{38}$$

with λ and ν being Lame's constant and Poisson's ratio. Therefore the flow of an incompressible Newtonian fluid can be modeled by the elastic deformation of an incompressible medium subjected to a body force.

In the present study, instead of solving the problem of an incompressible material, i.e., Eqs. (16a) and (37), we treat the material as nearly-incompressible. In other words, we approximate the problem by Eqs. (37) and (38) with ν nearly equal to 0.5. The specific value of
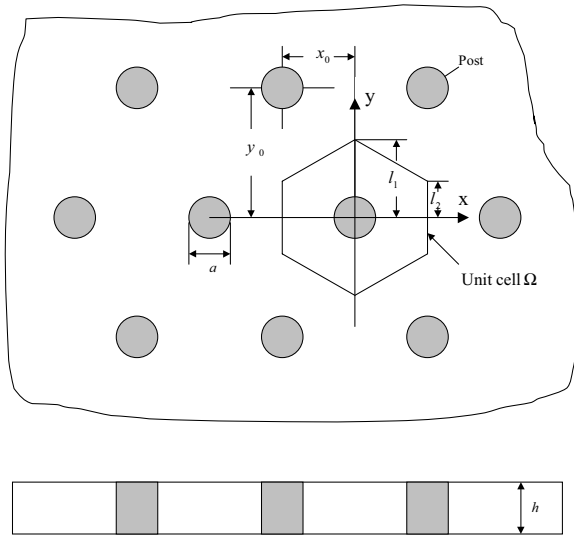
Figure 1 : Periodically distributed posts and unit cell

ν is determined by numerical experimentation of letting $\nu \to 0.5$.

We use the finite element method to solve the elastic problem of the unit cell subjected to constant body forces $F_i = -\partial p^{(0)}/\partial X_i$, which is constant in the microscale coordinates. The boundary conditions are zero displacements on the membranes at $z = \pm h/2$ and on the walls of the post Γ. The periodic condition required that the displacements and traction on the opposite sides of the hexagon be equal. The periodic displacement requirement is enforced simply by setting the degrees of freedom for nodes on corresponding sides to be the same (Tong and Mei, 1992). In general the periodic traction condition is implied by the way the degrees of freedom for the nodes on the cell boundaries are selected. The traction condition is satisfied only in mean in the finite element method. There are three independent constants for F_i. This means we have to solve the finite element equations three times, one for each of the independent constant. In the present study, we consider only the case $F_3(= -\partial p^0/\partial Z) = 0$ that there are only two independent constants. Once the average displacement $\left\langle u_i^{(0)} \right\rangle$ is obtained from the finite element solution, the permeability K_{ij} is easily found from Eq. (29), which is the function of μ/h^2, y_0/x_0, h/a and VSTR.

As an illustrative example, we consider a special case of regular hexagon cell (Fig. 1) with $y_0/x_0 = \sqrt{3}, a = 6.43\mu$m. We will examine K_{ij} for different combinations

of h/a and VSTR (vascular-space tissue ratio). The average displacement $\left\langle u_i^{(0)} \right\rangle$ in the unit cell is calculated under unit body force using the commercially available program ANSIS 5.6. The base of the hexagon cell is divided into 150 8-node quadrilateral elements and then extruded along $z-$axis to build (number of elements in the z-direction) of 20-node hexahedral elements. We have examined the convergence of the present calculation by reducing the current element size to 1/2 and 1/3 of the original element size and found litter changes in the results. We have also investigated the effect of incompressibility. The average displacement in the cell approaches to a stable value when Poisson's ratio is between 0.49990-0.49996. For Poisson's ratio too close to 0.5, the solution deteriorates due to round-off error. Thus Poisson's ratio equal to 0.4999 is used to assure a nearly incompressible deformation.

Table 1 gives the calculated K_{ij} for pure blood plasma flow without red blood cell ($\mu = 1.2 \times 10^{-3}$Ns/m^2) for h/a= 1, 2, 3, 4, 5, $y_0/x_0 = \sqrt{3}$ (regular hexagon) and VSTR=0.90. The numerical results indicate that $K_{11} \cong K_{22}$ and $K_{12} = K_{21} \cong 0$. This can be expected for a regular hexagonal cell that it should be transversely isotropic. That means the flow is insensitive to the flow direction in the x_1, x_2-plane. The values of K_{12} and K_{21} are much smaller than that of K_{11}, K_{22} and can be taken to be zero in practice. Thus the average flows along two orthogonal directions are decoupled. In Table 1, e denotes the maximum absolute value of volumeric strains in the cell. The vanishing values of e indicate that the deformations in the cell is nearly incompressible which assures the validity of the calculation.

Figure 2 shows the variation of K_{11} normalized by K^0 with increasing ratio of sheet thickness to post diameter h/a, for different values of VSTR. The constant $K^0(= \frac{h^2}{12\mu})$ is the permeability for the Couette flow (the case without posts and VSTR=1). The figure shows that for lower VSTR value, the permeability K_{11} is also lower. The ratio K_{11}/K^0 decreases with increasing h/a, which indicates increasing flow resistance for fixed K^0. In other words, permeability decreases (harder to flow) as the post diameter decreases for fixed vascular-space tissue ratio and channel height. For the post configuration considered, with the post volume of 4.5% of the cell, K_{11}/K^0 changes from 0.8 to about 0.3 as the sheet gap to post diameter ratio (h/a) increases from 1 to 5. The figure also reveals that the lower the vascular-space tissue ratio is,

	h / a = 1	h / a = 2	h / a = 3	h / a = 4	h / a = 5
$K_{11} = K_{22}$ (m^4/Ns)	1.78×10^{-8}	4.47×10^{-8}	6.30×10^{-8}	7.39×10^{-8}	8.07×10^{-8}
$K_{12} = K_{21}$ (m^4/Ns)	3.60×10^{-20}	9.95×10^{-20}	2.92×10^{-20}	7.61×10^{-20}	1.40×10^{-20}
e	1.73×10^{-8}	3.09×10^{-8}	4.04×10^{-8}	4.59×10^{-8}	4.11×10^{-8}

Table 1 : Calculated K_{ij} for pure blood plasma flow ($\mu = 1.2 \times 10^{-3}$Ns/m^2, VSTR=0.90, $y_0/x_0 = 1.732$)
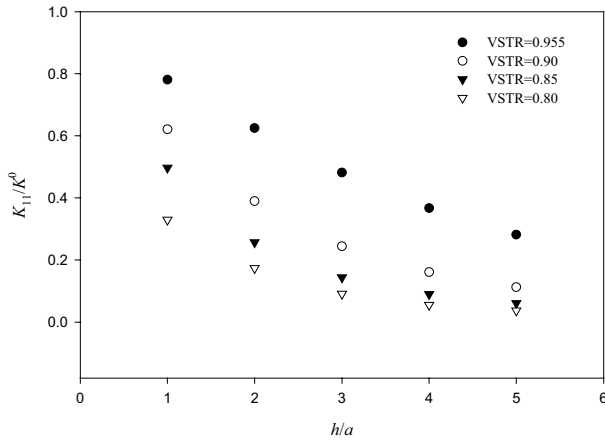

Figure 2 : Variation of K_{11}/K^0 with h/a for regular hexagon ($y_0/x_0 = 1.732$)
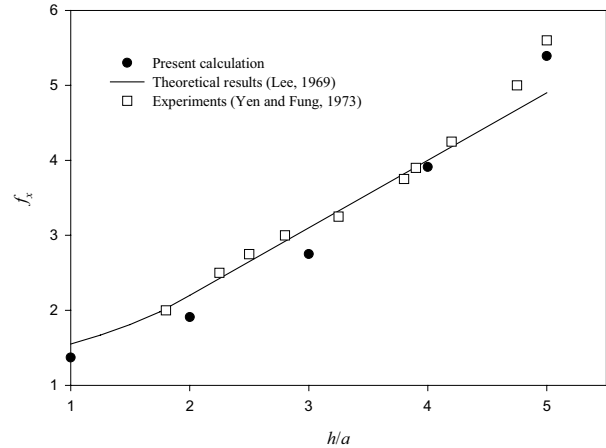

Figure 3 : Comparison of theoretical and experimental results for elongated hexagon ($y_0/x_0 = 3.99$, VSTR=0.955)

the lower the permeability K_{11}. This means that it is also more difficult for the blood to flow through a sheet with denser posts (lower VSTR). The relationship is nonlinear. At VSTR = 0.955 with $h/a = 5$, i.e. the posts occupy only 4.5% of the vascular-space, the value of K_{11}/K^0 is less than 0.3 and for VSTR = 0.8, the value is less than 0.05.

Next we consider the case of a non-regular hexagon (elongated in the y- direction) with

$y_0/x_0 = 3.99$, $a = 0.643$cm, VSTR=0.955, $\mu = 5$N s/m^2.

This is configuration used by Yen and Fung (1973) to experimentally determine the geometric frictional factor f_x. Table 2 gives K_{11}, K_{22}, K_{21} and K_{12} for the case of elongate hexagonal cell when h/a=1, 2, 3, 4, 5.

The calculated results also show that $K_{11} \neq K_{22}$. Clearly the elongated hexagonal cell is no longer transversely isotropic, which means the flow is sensitive to the flow direction in the x_1, x_2-plane. The calculated K_{12} and K_{21} are practical zero as compared to K_{11} and K_{22}, which

means the average flows along two orthogonal directions are decoupled.

Accordingly, the geometric frictional factors, f_x and f_y are proportional the reciprocals of K_{11}/K^0 and K_{22}/K^0, respectively. From Eq. (34)

$$f_x = \frac{h^2}{\mu \eta K_{11}} = \frac{12}{\eta} \frac{K^0}{K_{11}}, \quad f_y = \frac{h^2}{\mu \eta K_{22}} = \frac{12}{\eta} \frac{K^0}{K_{22}}, \quad (39)$$

because $K_{21} \cong K_{12} \cong 0$. Figure 3 plots the calculated f_x vs. the ratio of sheet thickness to post diameter h/a. For comparison, the figure also gives the experimental results of Yen and Fung (1973) as well as the theoretical predictions of Lee (1969). The present calculated results are reasonable fittings with Yen and Fung's experimental data. However, our results are noticeably different from Lee's theoretical results. This is probably because Lee's theoretical prediction is based on an approximate solution valid only for h/a not much larger than unity.

Figure 4 depicts the variation of the normalized per-

	$h/a = 1$	$h/a = 2$	$h/a = 3$	$h/a = 4$	$h/a = 5$
K_{11} (m⁴/Ns)	5.02×10^{-7}	1.45×10^{-6}	2.25×10^{-6}	2.82×10^{-6}	3.20×10^{-6}
K_{22} (m⁴/Ns)	5.45×10^{-7}	1.85×10^{-6}	3.45×10^{-6}	5.02×10^{-6}	6.38×10^{-6}
K_{21} (m⁴/Ns)	6.88×10^{-16}	6.80×10^{-15}	2.07×10^{-14}	3.82×10^{-14}	5.54×10^{-14}
K_{12} (m⁴/Ns)	7.42×10^{-16}	7.02×10^{-15}	2.10×10^{-14}	3.85×10^{-14}	5.56×10^{-14}

Table 2 : Calculated K_{ij} for elongate hexagonal cell ($y_0/x_0 = 3.99$, $a = 0.643$cm, VSTR=0.955, $\mu = 5$N s/m^2)
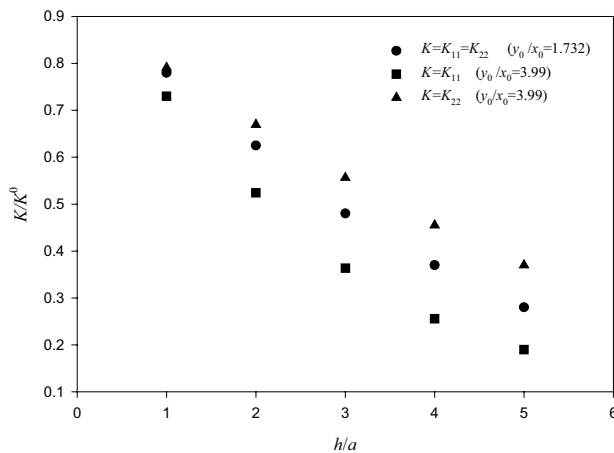

Figure 4 : Variation of K/K^0 with h/a under different hexagonal shapes (VSTR= 0.955)

meability K_{11}/K^0 and K_{22}/K^0 with h/a for two hexagonal cells of the same vascular-space tissue ratio (VSTR=0.955). One cell is the regular hexagon with $y_0/x_0 = 1.732$. In this care, $K_{11} = K_{22}$ and $f_x = f_y$. The other cell is an elongated hexagon with $y_0/x_0 = 3.99$. In this case, $K_{11} \neq K_{22}$ and $f_x \neq f_y$. The results indicate that $K_{11}(= K_{22})$ of the regular hexagon is bounded by K_{11} and K_{22} of the elongated hexagon. Thus, the shape of unit cell has an important influence on the permeability. In both cases, the permeability,K_{11} and K_{22}, decreases as h/a increases.

6 Conclusion

The sheet-flow model proposed by Fung and Sobin (1969) for blood flow in capillaries in the pulmonary alveoli is studied from micromechanical point of view. The pulmonary alveolar sheet is assumed to have a periodic microstructure of hexagonal cells. We use a two-scale theory of homogenization to establish the canonical equations for the unit cell. The microscale solution is obtained by the finite element method and the macroscopic pressure/discharge relationship for the flow in the pulmonary alveolar sheet is found through an average over the unit cell. Up to the order of $O(\varepsilon)$, the membrane can be treated as rigid and its motion can be neglected.

The cell geometry has an important effect on the permeability (geometric friction factor) of the macroflow. For regular hexagonal unit cell, the permeability tensor is diagonal and $K_{11} = K_{22}$ (i.e., geometric friction factor tensor is also diagonal and $f_x = f_y$). This means that the average flow is insensitive to the flow direction in the sheet plane. When the unit cell is an elongated hexagon, even though K_{ij} is still diagonal, the diagonal components are no longer equal ($K_{11} \neq K_{22}$, $f_x \neq f_y$) and the average flow is directional sensitive. Because K_{ij}, i.e., f_{ij}, is diagonal, the average flows along the x_1, x_2- directions are still decoupled.

The tissue posts make it more difficult for blood to flow through the two parallel sheets. When h/a is large, the flow resistance is mainly from the posts. The effect is quite nonlinear. Reducing either the post diameter or the vascular space tissue ratio will reduce permeability. For the post configuration considered, with the post volume of 4.5% of the cell, the ratio of the permeability to that of Couette flow (K_{11}/K^0) changes from 0.8 to about 0.3 when sheet gap to post diameter ratio (h/a) increases from 1 to 5. The reduction in permeability is even more pronounce for denser posts. At $h/a = 5$, K_{11}/K^0 is about 0.3 for the post volume of 4.5% of the cell. When the post volume increases to 20% of the cell, K_{11}/K^0 drops to 0.05. The tissue posts have a significant effect on the flow resistance.

References

Bush, A. W.(1992): Perturbation Methods for Engineers and Scientists. CRC, London.

Carvelli, V.; Maier, G.; Gastaldi, L. (2000): Kinematic limit analysis of periodic heterogeneous media. *CMES: Computer Modeling in Engineering & Sciences*, Vol. 1, pp. 19-30.

Fung, Y. C.; Sobin, S. S. (1969): Theory of sheet flow in lung alveoli. *J Appl Physiol*, Vol. 26, pp. 472-488.

Fung, Y. C. (1972): Theoretical pulmonary microvascular impedance. *Ann Biomed Eng*, Vol. 1, pp. 221-245.

Fung, Y. C.; Yen, R. T. (1986): A new theory of pulmonary blood flow in zone 2 condition. *J Appl Physiol*, Vol. 60, pp. 1638-1650.

Fung, Y. C. (1997): Biomechanics: Circulation. Springer-Verlag, New York.

Gao, J.; Huang, W.; Yen, R. T. (2000): Microcirculation impedance analysis in cat lung. *ASME J Biomech Eng*, Vol. 122, pp. 99-103.

Gan, R. Z.; Yen, R. T. (1994): Vascular impedance analysis in dog lung with detailed morphometric and elasticity data. *J Appl Physiol*, Vol. 77, pp. 706-717.

Huang, W.; Tian, Y.; Gao, J.; Yen, R. T. (1998): Comparison of theory and experiment of pulsatile flow in cat lung. *Ann Biomed Eng*, Vol. 26, pp. 812-820.

Kalamkarov, A. L. (1992): *Composite and Reinforced Elements of Construction*. Wiley, New York.

Lee, J. S. (1969): Slow viscous flow in a lung alveoli model. *J Biomechanics*, Vol. 2, pp. 187-198.

Mei, C. C.; Auriault, J. L.; Ng, C. O. (1996): Some applications of the homogenization theory. *Advances in Applied Mechanics*, Vol. 32, pp. 278-348.

Michel, J. C.; Moulinec, H.; Suquet, P. (2000): A computational method based on augmented Lagrangians and fast Fourier transforms for composites. *CMES: Computer Modeling in Engineering & Sciences*, Vol. 1, pp. 79-86.

Olman, M. A.; Gan, R. Z.; Yen, R. T.; Villespin, I.; Maxwell, R.; Pedersen, C.; Konopka, R.; Debes, J.; Moser, K. M. (1994): Effect of chronic thromboembolism on the pulmonary artery pressure-flow relationship in dogs. *J Appl Physiol*, Vol. 76, pp. 875-881.

Parton, V. Z.; Kudryavtsev, B. A. (1993): Engineering Mechanics of Composite Structures. CRC, London.

Tong, P.; Mei, C. C. (1992): Mechanics of composites of multiple scales. *Computational Mechanics*, Vol. 9, pp. 195-210.

Yen, R. T.; Fung, Y. C. (1973): Model experiments on apparent blood viscosity and hematocrit in pulmonary alveoli. *J Appl Physiol*, Vol. 35, pp. 510-517.

Yen, R. T.; Zhuang, F. Y.; Fung, Y. C.; Zeng, Y. J. (1984): Comparison of theory and experiments of blood flow in cat's lung. In: Y. C. Fung; E. Fukada; J. Wang (ed) Biomechanics in China, Japan and USA, Science, Beijing, pp. 240-253.

Yen, R. T.; Sobin, S. S. (1986): Pulmonary blood flow in the cat: correlation between theory and experiment. In: G. W. Schmid-Schönbein (ed) Frontiers in Biomechanics. Springer-Verlag, New York, pp. 365-376.

Zhuang, F. Y.; Fung, Y. C.; Yen, R. T. (1983): Analysis of blood flow in cat's lung with detailed anatomical and elasticity data. *J Appl Physiol*, Vol. 55, pp. 1341-1348.